AN APPROXIMATED CURVE HYSTERETIC SIMULATION MODEL FOR SEISMIC RESPONSE OF STEEL BRIDGE PIERS

Ji DANG[1] and Tetsuhiko AOKI[2]

[1]Department of Civil and Earth Resources Engineering, Kyoto University, Kyoto 615-8540, Japan
Email: dang.ji.5e@kyoto-u.ac.jp
[2] Department of Urban and Environment, Aichi Institute of Technology, Toyota 470-0392, Japan
Email: aoki@aitech.ac.jp

ABSTRACT

In this paper, an approximated curve hysteretic model is proposed to predict the seismic response of steel piers under strong ground motion. Instead of multiple straight lines, a series of curves are adopted to descript the complicated force-displacement hysteretic relationship of steel piers. P-δ effect, hardening effect in unloading-reloading hysteretic loops, deterioration characters of steel columns are considered in this model by introducing hysteretic rules and identifying free parameters. To verify the accuracy of the proposed model, six static cyclic tests and eleven hybrid tests using three types of steel pier specimens are conducted under the six strong ground motion records. By comparing the results due to the hybrid tests and the simulation, the average difference between these two is clarified as 5% in maximum response displacement, 22% in residual displacement and 3% in energy absorption.

INTRODUCTION

In the Kobe earthquake Japan of 1995, the collapse of steel bridge piers cost extremely large due to delay of the urgent support and loss of function of transportation. To maintain the function of urban high-way road after attacks of strong ground motions, the seismic performance of viaduct bridge piers has been considered as one of the most important issues.

Great amount of monotonic and quasi-static loading tests (Usami et al, 1991, 1992, 1993; Suzuki et al, 1995; Ge et al, 1997; Aoki et al, 2007) have been conducted to clarify the seismic performance of steel bridge piers to date. By conducting seismic response loading hybrid tests and simulation study (Usami et al, 1995; Aoki et al ,1998), it has been found that the seismic response of steel bridge piers is influenced the hysteretic character due to material and geometrical non-linear behavior as well as the uncertainty of ground motions.

Many seismic response simulation analysis techniques have been developed for steel bridge piers. The single degree of freedom model simulation (SDOF) applying experiment phenomenological load-displacement hysterical rules models has been recognized as most practically effective and efficient technique in both seismic response based design and studies which need seismic response results in great quantity.

A lot of efforts have been made to develop viable hysteretic model for SDOF simulation of steel piers. One representative example is the 2-parameter model (Suzuki et al. 1996) which is a stiffness softening considered tri-linear type hysteretic model using two lines to simulate the hysteretic behavior before peak load and linear deterioration post peak. Another tri-linear type hysteretic model, namely damage-based model (Kindaichi, 1998), introduced damage index to evaluate the force deterioration and stiffness softening of steel piers. Hybrid tests results for pipe section steel piers have been conducted and used to compare and verify these two hysteretic models (Liu et al, 2001), and difference in response by these two hysteretic model were found very large when a Kobe earthquake record, namely JR Takatori, was input as excitation, though this difference is small due to using records JMA or HKB. Both above two hysteretic models can be considered as practically effective models. However, the reason of unstable in response displacements for some earthquake is left as future works.

The tri-linear type hysteretic models are practically easy due to simplifying the hysteretic curve to tree lines. The detail information of load-displacement relation as well as the authenticity of response results, however, will be partly decreased by this simplification. It would be preferable that the hysteretic model can be more detailed and high-reality in load-displacement relation prediction.

In this study, a hysteretic model applying a serious of smooth curves to approximate the hysteretic load-displacement relationship is proposed to simulate the hysteretic character and none-linear seismic response for steel bridge piers. The load-displacement relationship is in essence approximated by cubic type basic curve, and simplified quadratic type sub-curve is used to present the hardening effect caused by unloading-reloading hysteretic. The concept of cumulative

deterioration displacement is introduced to evaluate the damage of steel piers caused by local buckling and to predict the degrading of the strength and stiffness. The relationship of distance of peak load points and cumulative deterioration displacement is also discussed.

To verify the validity of this approximated curve hysteretic model, a series of quasi-static tests and hybrid tests are conducted using stiffened square-section steel bridge pier specimens under the six uni-directional strong ground motion recordings prescribed by road bridge seismic design specification of Japan (Japan Road Association, 2002b). By comparing the result due to tests and numerical analysis, the validity of the proposed method is clarified accurately in the seismic response simulation.

THE APPROXIMATED CURVE HYSTERETIC MODEL

The equivalent horizontal force H_{eq}

To consider the $P-\delta$ effect of column under vertical axial force and horizontal loading, the relationship of horizontal force H and displacement δ are replaced by the relationship of equivalent horizontal force H_{eq} and displacement δ. As shown in Fig.1, the moment at the base of the column M_B, which combines the moment caused by horizontal force H and the moment caused by axial force P, can be expressed by equation (1).

$$M_B = Hh + P\delta \tag{1}$$

And the equivalent horizontal force is defined as horizontal force acting at the height h to present the base moment M_B which contains the $P-\delta$ effect.

$$H_{eq} = M_B/h = H + P\delta/h \tag{2}$$

Outline of curve approximated hysteretic model

The hysteretic loops expressed by $H_{eq}-\delta$ relation of steel piers are approximated by (A) basic curve, (B) sub curve and (C) deterioration curve, as presented in Fig.2. The basic curve starts at the beginning point of loading or an unload point in former basic curve and ends at a peak load point, as can be seen in Fig.2. This curve is used to draw out the skeleton $H_{eq}-\delta$ curve in the elastoplastic region before the peak load point. The sub curve connects two unloading points and can be used to approximate the hardening portion of a hysteretic loop when the pier is reloaded back to a former loading path. Or it also can be used to approximate hysteretic loops when the amplitude of loading is gradually reducing so the residual response displacement can be calculated properly. The deterioration curve, which starts from a peak load point, is introduced to express the reducing of horizontal force when the steel panel starts and continuously deteriorates due to local buckling.

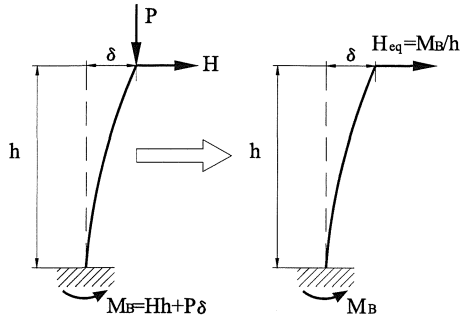

Figure 1. Definition of equivalent horizontal force H_{eq}

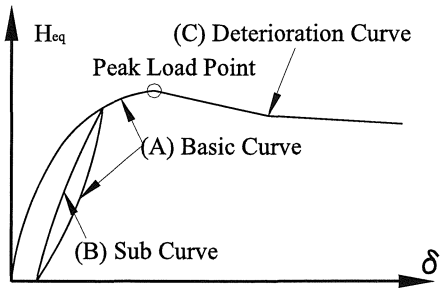

Figure 2. Outline of curve approximated model

The basic curve

A hysteretic equivalent horizontal force-displacement relation of steel piers contains a serious of half loading loops. In each half loading loop without deterioration, the $H_{eq}-\delta$ relation can be approximated by a basic curve which is expressed by the following equation.

$$H_{eq} - H_s = K_e(\delta - \delta_s) + \alpha_1(\delta - \delta_s)^2 + \alpha_2(\delta - \delta_s)^3 \tag{3}$$

In the above equation, δ_s and H_s means the displacement and equivalent horizontal force of the start point of this half loop, respectively. For the initial half loop, as indicated 1 in Fig.3, the start point is the origin O. For a general half loop

i, the start point is the unload point of the former half loop i-1. For example, the start point of the second half loop 2 indicated in Fig.3, is the point A, where the half loop 1 reversed.
The parameter K_e in the above equation is the elastic stiffness of the steel piers. It expresses the initial slope of a basic curve in its start point. The parameters α_1 and α_2 determine the shape of the approximated curve and express how the slope of a basic curve degrading from the elastic stiffness K_e to the slope at the target point of this basic curve (δ_t,H_t). Usami T. [1]~[3], Suzuki M. [7] and Iura M. [14] have pointed out in their tests that the normalized peak loads H_m and the corresponding displacements δ_m of steel piers can be considered as a value which are only involved with the geometry and material parameters of the piers but not depend on the loading history. Therefore, the peak load points in positive and negative loading sides, which are referred as (δ_m, H_m) and ($-\delta_m$,$-H_m$) in Fig.3, can be recognized as temporarily constant target points of basic curves. The slope of basic curve at peak points (δ_m, H_m) or ($-\delta_m$,$-H_m$) should be 0, because the slope of hysteretic loop change from positive to negative at these points. Then, the value of α_1 and α_2 can be determined by the following equations.

$$\alpha_1 = 3(H_t - H_s)/(\delta_t - \delta_s)^2 - 2\,K_e/(\delta_t - \delta_s) \quad (4)$$
$$\alpha_2 = K_e/(\delta_t - \delta_s)^2 - 2(H_t - H_s)/(\delta_t - \delta_s)^3 \quad (5)$$

In the above equation, (δ_t, H_t) presents the target peak loop points in positive or negative direction. For example, the target point (δ_t, H_t) of curve 1 in Fig.3, which is a basic curve directing in positive direction, is the peak load point of positive direction (δ_m, H_m), and the target point (δ_t, H_t) of curve 2 in Fig.3, which is a basic curve directing in negative direction, is the peak load point of negative direction ($-\delta_m$,$-H_m$).

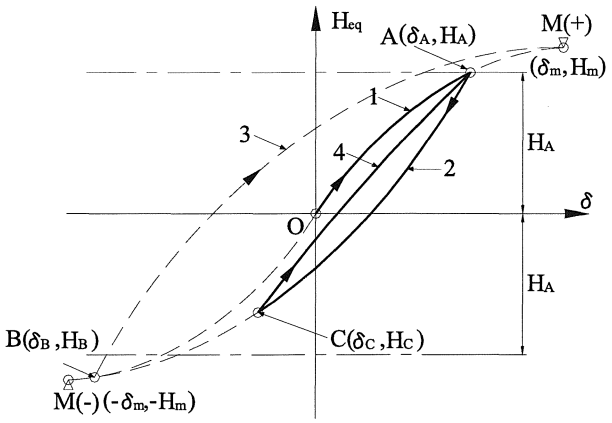

Figure 3. Basic curves and sub curves

The sub curve

An unloading point of one hysteretic curve is also the start point of the next curve. Point A in Fig.3, for example, is an unloading point of curve 1 and also the start point of curve 2. Once the proceeding direction reversed, a new hysteretic curve should be pre-established by applying the unload point ($\delta_{u,p}$, $H_{u,p}$) of present curve, which is also the start point of next new curve ($\delta_{u,n}$, $H_{u,n}$), and the target point ($\delta_{t,n}$, $H_{t,n}$). The new curve could be pre-established as a basic curve by equation (3), (4) and (5), if the condition of following equation is satisfied.

$$(H_{u,p} - H_{s,p}) \times \mathrm{sgn}(\delta_{u,p} - \delta_{s,p}) > 2H_{s,p} \quad (6)$$

Where sgn() is the sign function which is defined as sgn(x) = 1 when x > 0, and sgn(x) = -1 when x < 0, and ($\delta_{s,p}$, $H_{s,p}$) is the start point of the present curve. The above condition equation presents that the loading amplitude is gradually ascending to higher plastic level, like unloading at point A from curve 1 and unloading at point B from curve 2. As the equation (6) can be rewrite as $(H_A - 0)\mathrm{sgn}(\delta_A - 0)>0$, the next curve 2 in the figure, is pre-established as a basic curve. Similarly, unloading from point B from curve 2 will lead a new basic curve 3.
If the condition presented by equation (6) is no satisfied, like a case unloading occurs from point C in the figure, the next hysteretic curve is effected strongly by the former loading loop. So, the loading path will lead hysteretic curve back to the former unload point A and then go forward along the curve path of the former loading continuously, like the path of curve 4 to curve 1 passing through point A in the figure. The loading path connecting two unload points like curve 4 can be approximated by degenerating the equation (3) simply to a quadratic form by setting the parameter α_2 =0 and calculating the parameter α_1 by following equation.

$$\alpha_1 = (H_t - H_s)/(\delta_t - \delta_s)^2 - K_e/(\delta_t - \delta_s) \quad (7)$$

Here the (δ_t, H_t) and (δ_s, H_s) present the target and start point of next curve, respectively, as same in equation (4) and (5), which is point A and point C for curve 3.
On the other hand, after unloading from a sub curve, the next curve from the unload point should be a new sub curve. The above hysteretic rules can be summarized as a flowchart presented in Fig.4.

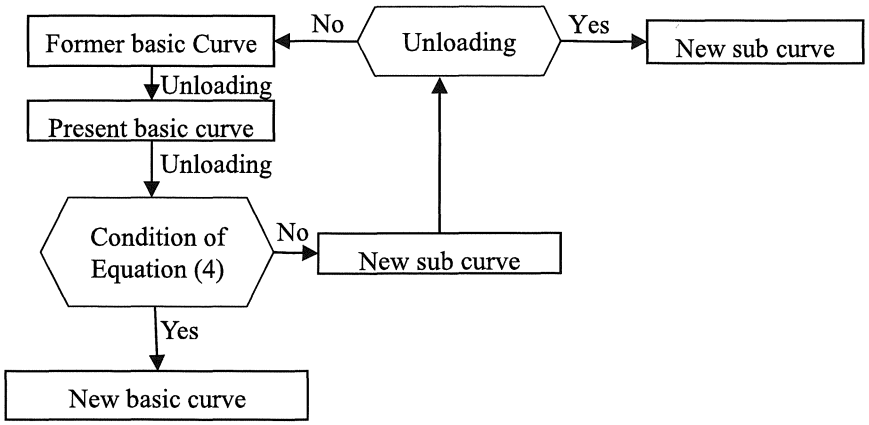

Figure 4. The flow chart of hysteretic rules in curve selection

The cumulative deterioration displacement (CDD)

Fig.5 shows a half cyclic hysteretic curve showing a deterioration part. The deterioration starts from the peak load point $M(\delta_m, H_m)$ and ends at the unloading point $U(\delta_u, H_u)$. The displacement length experienced in this deterioration part can be expressed as $\delta_p = \delta_u - \delta_m$. Denote the deterioration displacement experienced in the i^{th} cycle as $\delta_d^{(i)}$. After n cycles, once the displacement go further than the displacement at the peak load of the present cyclic (δ_m), the cumulative deterioration displacement $\sum \delta_d$ is updated by the following equation using the present displacement δ.

$$\sum \delta_d = \sum |\delta_d^{(i)}| + |\delta - \delta_m| \quad (8)$$

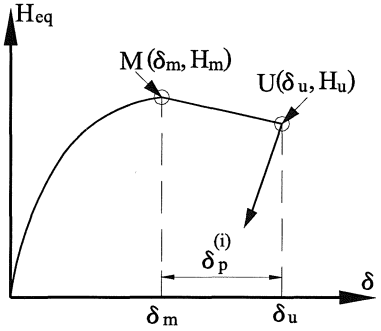

Figure 5. Deterioration displacement

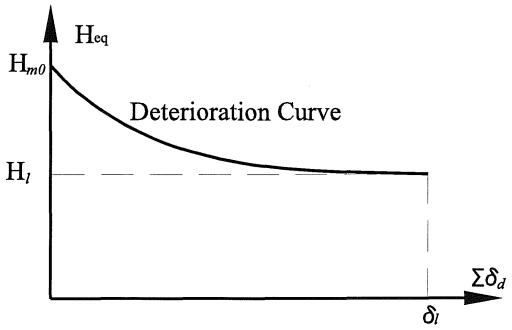

Figure 6. Deterioration Curve

The deterioration curve

A quadratic equation is proposed as following equation to describe the relationship between the equivalent horizontal force H_{eq} and the cumulative deterioration displacement $\sum \delta_d$,

$$H_{eq} = H_{m0} + (H_{m0} - H_l)(\sum \delta_d / \delta_l - 2) \sum \delta_d / \delta_l \quad (7)$$

where H_{m0} is the initial value of peak load, δ_l and H_l are defined as the limit point of deterioration of strength, as can be seen in Fig.6, where the H_{eq} hit its bottom limit value H_l when the cumulative deterioration displacement $\sum \delta_d$ hit a limit value δ_l. The exact value of δ_l and H_l can be determined by the least-squares method from the quasi-static loading test data hereafter.

The deterioration of elastic stiffness

After experienced deterioration of load, the unloading elastic stiffness K_e is generally lower than its initial value K_{e0}. The degree of stiffness degrading is normally associated with the cumulative damage caused by the local buckling. Flowing linear equation can be applied for evaluation of deterioration of elastic stiffness K_e after cumulative deterioration displacement $\sum \delta_d$ is experienced.

$$K_e/K_{e0} = 1 - \kappa \sum \delta_d / \delta_l \tag{8}$$

where K_{e0} is the initial elastic stiffness, and the free parameter κ is used to express the rate of stiffness deterioration of stiffness when the deterioration displacement is cumulated to limit value δ_l. The exact value of κ will be discussed by the quasi-static test conducted hereafter.

Variation of peak load points due to deterioration

After some deterioration has experienced in one of two loading directions, both peak load points in this two loading directions are changed to new force-displacement locations, as can be seen in the example shown in Fig.7. The new peak load point M'_1 in the direction of deterioration should be the unload point on the present deterioration curve, as can be seen in Fig.7. So that the peak load point of deteriorated direction is updated to point M'_1 instead of old peak load point M_1.

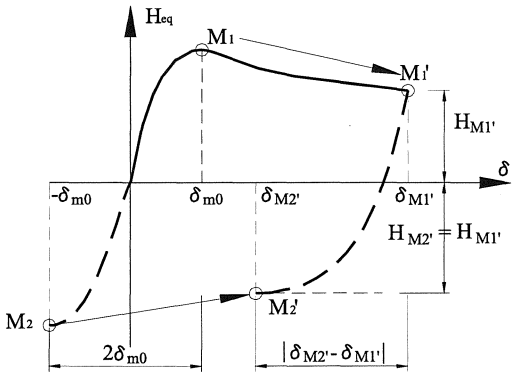

Figure 7. Hysteretic rules after deterioration

In the opposite direction, affected by the deterioration loading experienced in another direction, the peak load post deterioration should be lower than its initial value. Therefore, the peak load point should be updated to M'_2 from M_2, though there were no deterioration experienced at all in this direction. As a simplified assumption, the residual strength of both directions can be approximately considered as descending simultaneously during the deterioration loading. Thus the peak load of the opposite direction $H_{M2'}$ should be as same as the new peak load of deteriorated direction.

$$H_{M2'} = H_{M1'} \tag{11}$$

The displacement $\delta_{m2'}$ of peak point M'_2, can be presumed by its distance of two new peak points $|\delta_{m2'} - \delta_{m1'}|$ which is generally increasing by the cumulative damage due to local buckling. Evaluating the damage by the cumulative deterioration displacement $\sum \delta_d$, the distance of new peak load points can be predicted by the following equation.

$$|\delta_{m2'} - \delta_{m1'}|/2\delta_{m0} = 1 + \gamma \sum \delta_d / \delta_l \tag{12}$$

where $2\delta_{m0}$ is the initial distance of two peak load points, and γ is a free parameter which will be identified from quasi-static tests hereafter.

PARAMETER IDENTIFICATIONS

As mentioned above, following free parameters should be identified before conducting the numerical simulation.

I. Initial peak load point (δ_{m0}, H_{m0})

II. The limit deterioration point (δ_l , H_l).

III. The parameter κ, which expresses the descending rate of elastic stiffness.

IV. The parameter γ, which expresses the expansion rate of distance between peak points in two loading directions.

Other variables involved above, e.g., δ_{m0}, H_{m0} and K_{e0}, can be obtained theoretically. To identify the appropriate value of these parameters, a serious of quasi-static loading tests were conducted for stiffened box-section steel bridge pier.

Quasi-static tests

Three types of test specimens, sharing same square-section but with different diaphragm stiffen, are used to conduct loading tests. All specimens are made by the steel with grade of SM490. Six mm thick steel plates are used to make 450mm width square section piers. There are two ribs back each surface of the box section. Three types of specimens, which have different diaphragm intervals of 450mm, 225mm and 150mm, are prepared and referred as D450, D225 and D150, respectively. Two specimens for each type are used for the cyclic loading tests. Figure 6 and Figure 7 shows the side views and the section view of specimens. The geometry sizes and parameters of specimens are listed in Table 1 and Table 2. The width-thickness ratio R_R, R_F and the length-to-slenderness ratio λ are calculated by following equations [15].

$$R_R = \frac{b}{t}\sqrt{\frac{\sigma_y}{E}\frac{12(1-v^2)}{\pi^2 k_R}} \tag{13}$$

$$R_F = \frac{b}{t}\sqrt{\frac{\sigma_y}{E}\frac{12(1-v^2)}{\pi^2 k_F}} \tag{14}$$

$$\lambda = \frac{2h}{r}\sqrt{\frac{\sigma_y}{E}} \tag{15}$$

$$k_R = 4n \tag{16}$$

$$k_F = \frac{(1+\alpha^2)^2 + n\gamma_l}{\alpha^2(1+n\delta_l)} \tag{17}$$

Table 1. Geometry sizes of specimens

Specimen	D450	D225	D150
b (mm)	450		
t (mm)	6		
b_S (mm)	55		
D (mm)	450	225	150
t_S (mm)	6		
h (mm)	2400		
A (mm^2)	13300		
I (mm^4)	4.06×10^8		

where α is the aspect ratio of the plate, α_0 is the limit aspect ratio, γ_l is supplement member's stiffness rate, δ_l is the area rate of one supplement member divided by whole section area, b and t are the width and thickness of each steel plate, r is the equivalent radiation of the cross section, h is the effective height of the test model pier, k_R, k_F are the buckling coefficient shown in Eq.(16) and (17) respectively.

Each specimen is subjected to the prescribed horizontal displacement pattern under a constant axial vertical load P of 0.15 times the squash load P_y (=4320 kN) which is obtained from the nominal yield stress of SM490.

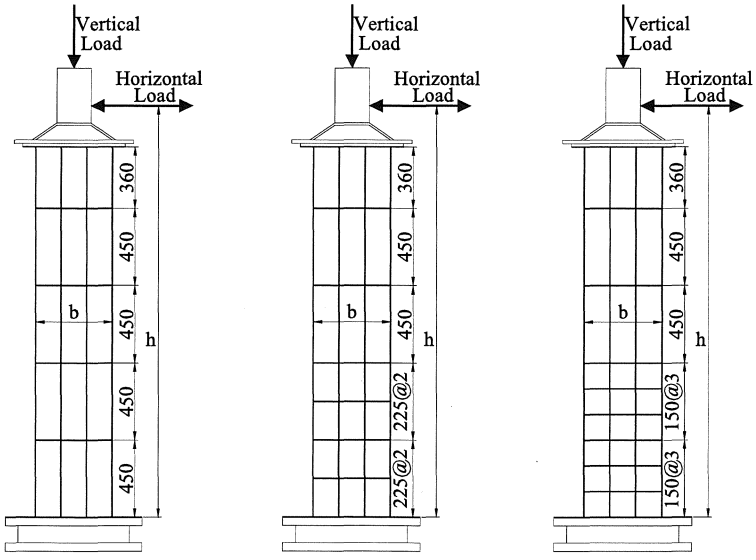

(a) Specimen D450 (b) Specimen D225 (c)Specimen D150

Figure 6. The side views of specimens

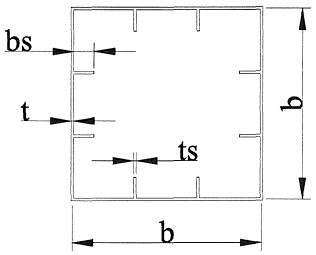

Fig.7 The section view

Table 2. Geometry parameters of specimens

Specimen	R_R	R_F	λ	λ_s	$\gamma/\gamma*$
D450	0.517	0.336	0.397	0.368	2.5
D225		0.170		0.183	10.5
D150		0.113		0.123	26.7

Parameter identification from quasi-static test results

Tensile coupon test are conducted for each pier specimen before their quasi-static tests, and the test results for each specimen type are listed in Table 3.

For each specimen type, two quasi-static tests are conducted, using the specimens named as D450-1, D450-2, D225-1, D225-2, D150-1 and D150-2. The yield displacement δ_y and yield force H_y are calculated by the measured yield strain. The initial elastic stiffness K_{e0} is obtained in average for each type. These are listed in Table 4.

Table 3. Result of material tests

Specimen	σ_y (N/ mm^2)	ε_y ($\times 10^{-6}$)	E (N/ mm^2)	σ_u (N/ mm^2)
D450	415	1961	2.25×10^5	568
D225	409	2011	1.98×10^5	546
D150	384	1858	2.07×10^5	505

Table 4. Hysteretic parameters from quasi-static tests

Specimen	δ_y (mm)	H_y (kN)	K_{e0} (kN/ mm)	δ_{m0}/δ_y	H_{m0}/H_y	δ_l/δ_y	H_l/H_y	κ	μ
D450	12.4	201	16.3	3.44	1.71	21.4	1.02	0.51	0.38
D225	15.0	238	15.9	2.57	1.71	13.3	1.11	0.04	0.13
D150	14.8	242	16.4	2.45	1.61	14.9	0.99	0.24	0.10

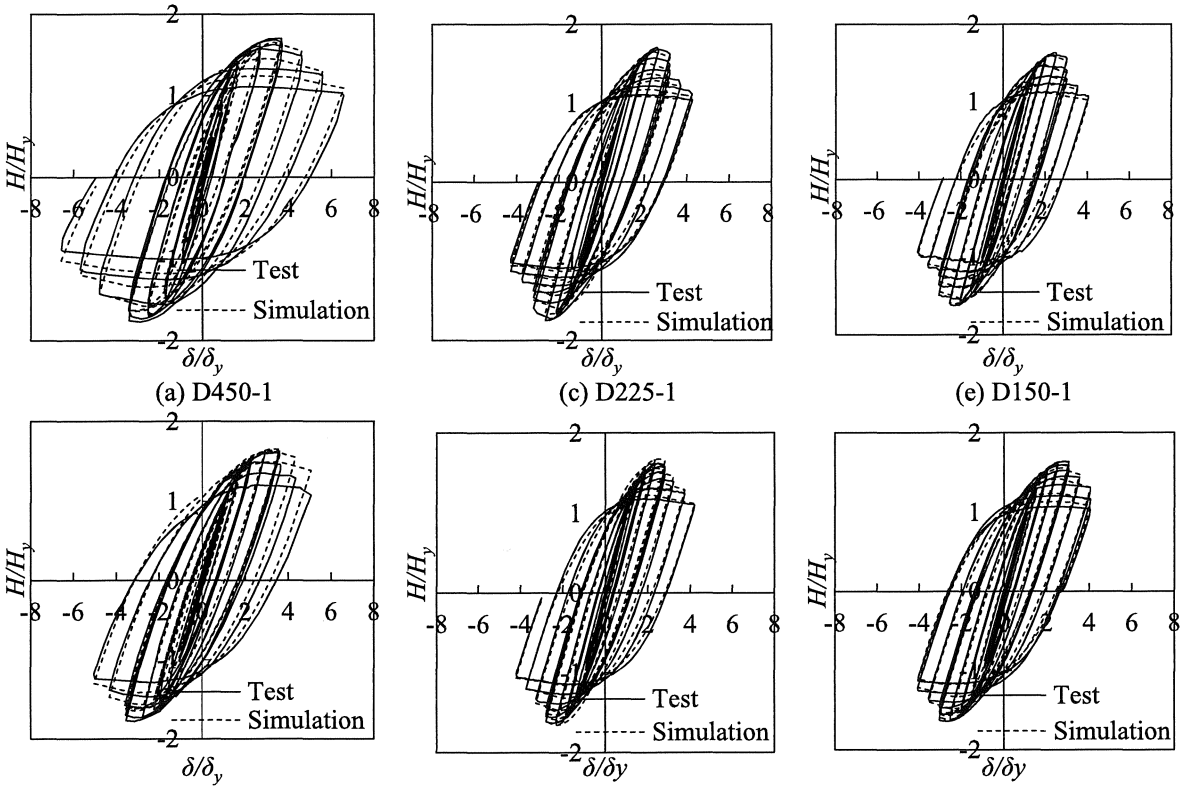

(a) D450-1 (c) D225-1 (e) D150-1

(b) D450-2 (d) D225-2 (f) D150-2

Figure 8. H-δ relation by cyclic loading tests and numerical simulation

In Figure 8 (a) ~ (f), the solid lines illustrate the H-δ loading history, where H and δ are normalized by H_y and δ_y respectively. From these figures, the initial peak load points (δ_{m0},H_{m0}) can be obtained as the average of two test results for same type of specimens as listed in Table 4.

By cumulating the displacement in deterioration region of each loading loop, the cumulative deterioration displacement $\sum \delta_d$ can be obtained for each loading test. The relationships between H_{eq} and $\sum \delta_d$ were plotted in Fig.9 (a)~(c). Approximated square equation curves and the first and second order parameters, referred as β_1 and β_2, can be obtain by the least square method from this H_{eq}-$\sum \delta_d$ relation data, the limit points (δ_l , H_l) can be calculated by substituting β_1 and β_2 into the following equations.

$$\delta_l = -0.5\beta_1/\beta_2 \quad (18)$$

$$H_l = H_{m0} - 0.25{\beta_1}^2/\beta_2 \quad (19)$$

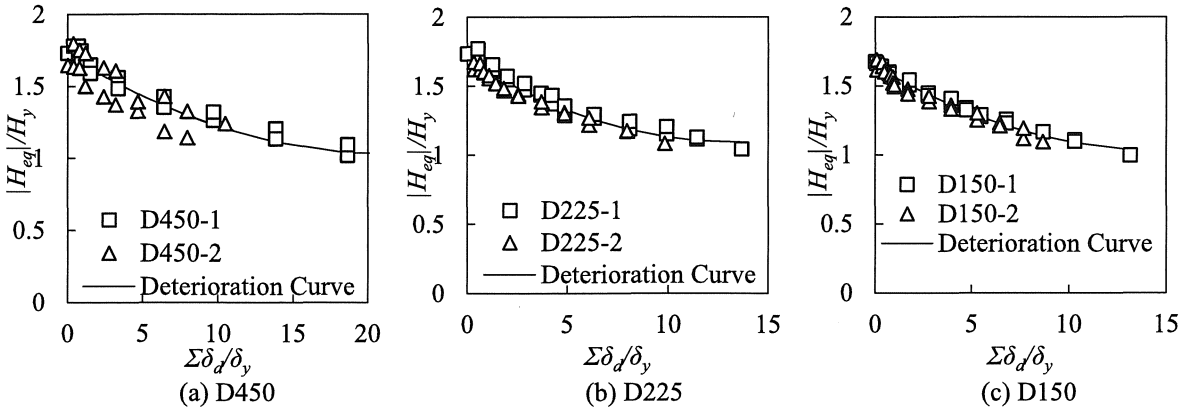

(a) D450 (b) D225 (c) D150

Figure 9. The relationships of H_{eq} and δ_d

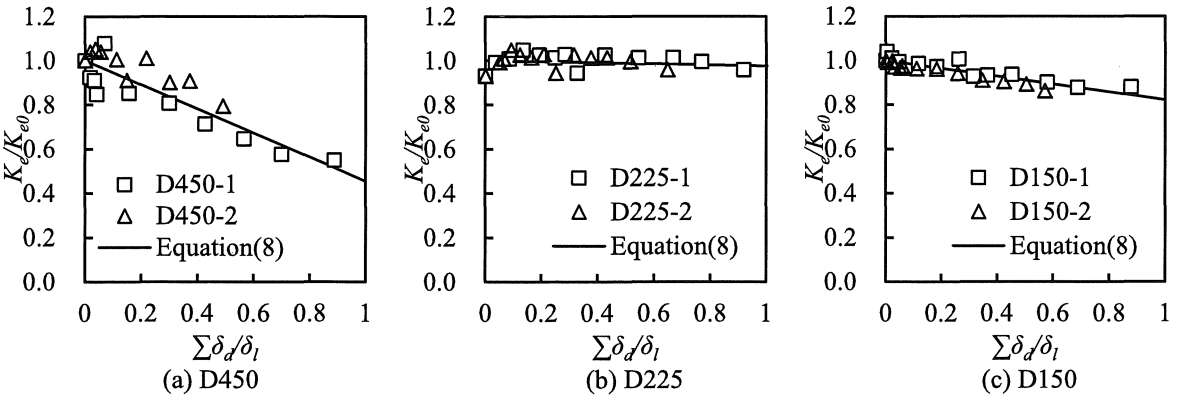

(a) D450 (b) D225 (c) D150

Figure 10. Deterioration of elastic stiffness

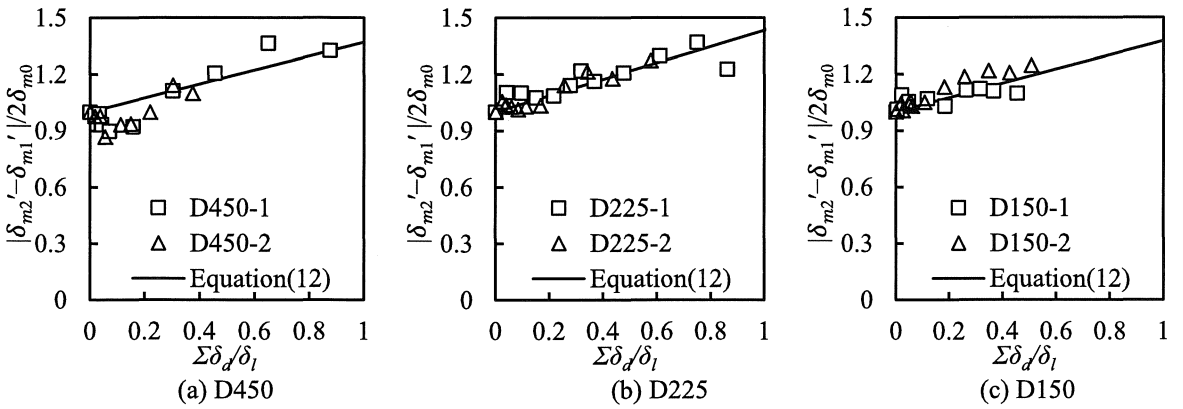

(a) D450 (b) D225 (c) D150

Figure 11. Expansion of peak load points distance after deterioration

The approximated deterioration curves are presented by solid lines in Fig.8, from these figures, approximate deterioration curves are found by applying Eq.(7), and the limit points (δ_l , H_l) are determined by the least-squares method and listed in Table 4.
By the same way, the stiffness deterioration K_e/K_{e0}-$\sum \delta_d/\delta_l$ and peak load point distance expansion $|\delta_{m2'} - \delta_{m1'}|/2\delta_{m0}$ -$\sum \delta_d/\delta_l$ obtained from quasi-static tests are plotted in Figures 10 and 11 respectively, and the regression value for parameter κ and γ are listed in Table 4.
After obtaining all necessary parameters, the H-δ loading histories were simulated and compared with the displacements history of the quasi-static tests, as shown by broken lines in Fig.8 (a) ~ (f). It can be seen from these figures that the results of simulation based on approximated curve hysteretic model are very similar to the loading tests.

VERIFICATION BY HYBRID TESTS

The hybrid loading tests are conducted to compare with the results obtained by proposed approximated curve model simulation for square-section steel bridge piers. The above mentioned specimens (D450, D225, D150) are used with the scale rate S=4 and 6 for real sized bridge piers. The Newmark β method (β=1/6) is applied to solve the vibration equation as a displacement prediction procedure using initial stiffness, under the time interval of Δt=0.01 sec and the damping ratio of 0.05 [16].
Hybrid tests and simulations are performed using six accelerograms of the Kobe Earthquake [13] in following three categories:

1)The NS and EW components recorded in Japan Meteorological Agency (JMA-NS, JMA-EW, Ground Type I);
2) The NS and EW components recorded in Japan Railway Takatori station (JRT-NS, JRT-EW, Ground Type II);
3) The NS and EW components recorded in Port-island Kobe Bridge (PKB-NS, PKB-EW, Ground Type III).

The program of the hybrid tests and simulations are listed in Table 5. The seismic response simulations are conducted by using the proposed approximated curve hysteretic model and parameters obtain by quasi-static tests. The hysteretic loops, response displacement time histories, maximum response displacements, residue displacements and energy absorptions obtained by hybrid loading tests are compared with those results by simulations as follows.

Table 5. Tests and Simulation Numbers and their Settings

Specimen Type	S	Excitation Accelerograms					
		JMA (Ground Type I)		JRT (Ground Type II)		PKB (Ground Type III)	
		NS	EW	NS	EW	NS	EW
D450	4	--	--	No.1	No.2	--	--
D450	6	--	--	--	No.3	--	--
D225	4	No.4	No.5	No.6	No.7	No.8	No.9
D150	4	--	--	No.10	No.11	--	--

The comparison of maximum response displacement
The maximum response displacement (δ_{max}) may be one of the most important indicators in the response performance based seismic design. The accuracy of an analysis method accounts mainly for the precision of the prediction of maximum response displacement of piers. Fig.13 shows the comparison in the maximum response displacement between tests and simulation. As can be seen, the maximum response displacements due to the simulations are almost as same as that of hybrid tests. The average error in maximum response displacement between simulations and hybrid tests is merely 5%, and the largest difference is less than $1\delta_y$.
The comparison of residual displacement
The residual displacement (δ_r) is a main indicator in estimation of the recovery capacity of the bridge pier after strong ground motion. Fig.14 shows the comparison of tests and simulations of residual displacement. Simulation predicted the tests results almost correct, with the absolute average discrepancy of only 22% or $0.35\delta_y$.
The comparison of energy absorption
Comparison in energy absorption of bridge pier between tests and simulations is indicated in Fig.15. The energy absorption due to the curve approximate hysteretic model provides almost as same results as that of the hybrid test. The average error is merely 3%.

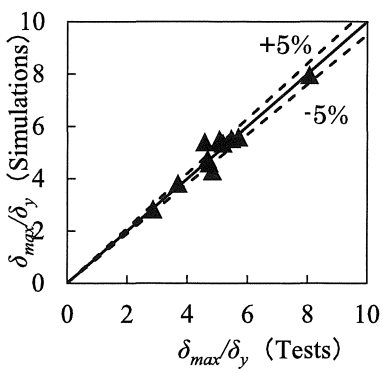

Figure 13. Comparison in δ_{max}

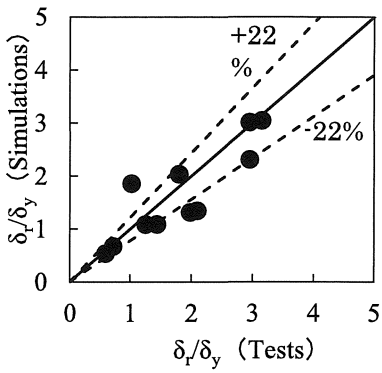

Figure 14. Comparison in δ_r

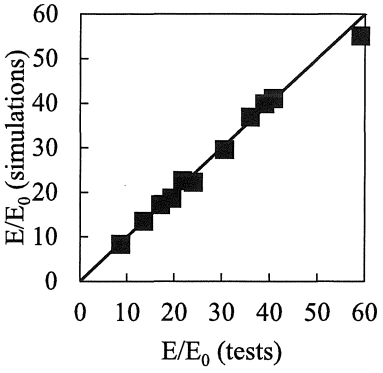

Figure 15. Comparison in E/E_0

SUMMARY AND CONCLUSIONS

In this study, the none-linear cyclic and deterioration behaviors of steel pier columns, such as the P-δ effect, constant initial peak load point character, unloading-reloading character, deterioration of strength and stiffness by cumulative deterioration, and expansion of distance between positive and negative peak load points are discussed. An approximated curve hysteretic model is proposed to express these behaviors of steel bridge pier columns. Based on the series of quasi-static and hybrid loading tests, the accuracy of seismic response simulation of the proposed approximate curve hysteretic model was discussed. It may be concluded from this study as follows.

(1) The P-δ effect is considered in the horizontal force-displacement relationship of steel pier columns. The first peak load point of steel pier can be considered as a constant point. The hysteretic loops before deterioration can be obtained by approximated basic curves based on the peak point. The unloading-reloading hardening character is taken into account by introducing sub curves so as to connect just before unloading points. The deterioration of strength and stiffness of steel piers is evaluated by counting the cumulative deterioration displacement. The distance expansion of peak loading points in two loading directions and stiffness softening are determined by the cumulative deterioration displacement.

(2) Parameters (δ_{m0}, H_{m0}), (δ_l , H_l), κ and γ are introduced to evaluate the non-linear hysteretic and deterioration behaviors of steel piers. The identification of these parameters for three types of square-section steel piers is conducted using quasi-static loading tests data.

(3) Eleven cases of hybrid loading tests were conducted using the same specimen as quasi-static tests. By comparing the response results of hybrid tests with the approximated curve hysteretic simulation model, it is clarified that the difference of maximum response displacement, residual displacement and energy absorption are 5%, 22% and 3%, respectively.

REFERENCES

Aoki,T., Ohnishi,A. and Suzuki,M. (2007): Experimental study on the Seismic Resistance Performance of Rectangular Cross Section Steel Bridge Piers subject to Bi-Directional Horizontal Loads" *Journal of Structural Engineering, JSCE*, Vol.63(No.4), 716-726.

Aoki,T., Suzuki,M. and Tanaka,T. (1998): Multi-Curve Model for Steel Pier Hysteretic Curve", *Proceedings of the Second Symposium on Nonlinear Numerical Analysis and its Application to Seismic Design of Steel Structures*, Vol.2, 271-274.

Iemura,H. (1985): Development and Future Prospect of Hybrid Experiments" *Structure Eng./Earthquake Eng., JSCE*, 356(I-3), 1-10.

Iura,M., Kumagai,Y. and Komaki,O.(1997): Ultimate Strength of Stiffened Cylindrical Shells Subjected to Axial and Lateral Forces, *Structure Eng./Earthquake Eng., JSCE*, No.556, 107-118

Japan Road Association (2002a): *Design Specifications of Highway Bridges (Part II. Steel Bridge).*

Japan Road Association(2002b): *Design Specifications of Highway Bridges (Part V. Seismic Design).*

Kindaichi T., Usami T., Satish K. (1998): A hysteresis model based on Damage Index for steel bridge piers" *Journal of Structure Engineer, JSCE*, Vol.53(A), 667-678.

Ge H.B., Gao S.B., Usami T., Matsumura T. (1997): Numerical Study on Cyclic Elasto-Plastic Behacior of Steel Bridge Piers of Pipe-Sections Without Stiffeners, *Structure Eng. / Earthquake Eng., JSCE*, No.577(I-41),

181-190.
Liu Q.Y., Kasai A., Usami T.(2001): Two hysteretic models for thin-walled pipe-section steel bridge piers, *Engineering Structures*,Vol. 23, Nov 2, 2001, 186-197.
Sibata, M. (2003): *Latest Seismic Resistance Analysis*, Morihaku Press.
Saizuka, K., Itoh, Y., Kiso,E. and Usami,T. (1995): A Consideration on Procedures of Hybrid Earthquake Responses Test taking account of the Scale Factor, *Structure Eng. / Earthquake Eng., JSCE*, No.505(I-30), 179-190.
Suzuki,M., Usami,T. and Takemoto,K. (1995): An Experimental study on Static and Quasi-Static Behavior of Steel Bridge Pier Models, *Structure Eng./Earthquake Eng., JSCE*, No.505(I-103), 99-108.
Suzuki,M., Usami,T., Terada M., Itoh, T. and Saizuka,K. (1996): Hysteresis Models for Steel Bridge Piers and their Application to Elasto-Plastic Seismic Response Analysis, *Structure Eng. / Earthquake Eng., JSCE*, No.549(I-37), 191-204.
Usami,T., Imai,Y, Aoki,T. and Itoh Y.(1991): An Experimental study on the Strength and Ductility of Steel Compression Member under Cyclic Loading, *Journal of Structure Engineer, JSCE*, 37(A), 93-106.
Usami,T., Mizutani,S., Aoki,T., Itou Y. and Yasunami, H.(1992): An Experimental study on the Elasto-Plastic Cyclic Behavior of Stiffened Box Members, *Journal of Structure Engineer, JSCE*, 38(A), 105-117.
Usami,T., Banno,S., Zetsu,H. and Aoki,T. (1993): An experimental study on the Elasto-Plastic Behavior of Compression Members under Cyclic Loading –Effect of Loading Program, *Journal of Structure Engineer, JSCE*, 39(A), 235-247.
Usami,T., Saizuka,K., Kiso,E. and Itoh, Y. (1995): Pseudo-Dynamic Tests of Steel Bridge Pier Model under Severe Earthquake, *Structure Eng./Earthquake Eng., JSCE*, No.519(I-32), 101-113.
Usami, T. (ed.) (2006): *Guidelines for Seismic and Damage Control Design of Steel Bridges*, Gihodo Shuppan (in Japanese).